

Volume-Activated Chloride Currents in Fetal Human Nasopharyngeal Epithelial Cells

Xuerong Sun · Lixin Chen · Haibing Luo ·
Jianwen Mao · Linyan Zhu · Sihuai Nie ·
Liwei Wang

Received: 16 September 2011 / Accepted: 31 January 2012 / Published online: 21 February 2012
© Springer Science+Business Media, LLC 2012

Abstract Volume-activated chloride channels have been studied by us extensively in human nasopharyngeal carcinoma cells. However, the chloride channels in the counterpart of the carcinoma cells have not been investigated. In this study, volume-activated chloride currents ($I_{cl,vol}$) were characterized in normal fetal human nasopharyngeal epithelial cells using the whole-cell patch-clamp technique. Under isotonic conditions, nasopharyngeal epithelial cells displayed only a weak background current. Exposure to 47% hypotonic solution activated a volume-sensitive current. The reversal potential of the current was close to the calculated equilibrium potential for Cl^- . The peak values of the hypotonicity-activated current at +80 mV ranged from 0.82 to 2.71 nA in 23 cells. Further analysis indicated that the

density of the hypotonicity-activated current in most cells (18/23) was smaller than 60 pA/pF. Only five cells presented a current larger than 60 pA/pF. The hypotonicity-activated current was independent of the exogenous ATP. Chloride channel inhibitors ATP, tamoxifen and 5-nitro-2-(3-phenylpropylamino) benzoic acid (NPPB), inhibited the current dramatically. The anion permeability of the hypotonicity-activated chloride channels was $I^- > Br^- > Cl^- > gluconate$. Unexpectedly, in isotonic conditions, ATP (10 mM) activated an inward-rectified current, which had not been observed in the nasopharyngeal carcinoma cells. These results suggest that, under hypotonic challenges, fetal human nasopharyngeal epithelial cells can produce $I_{cl,vol}$, which might be involved in cell volume regulation.

X. Sun

Institute of Aging Research, Key Laboratory for Medical Molecular Diagnostics of Guangdong Province, Guangdong Medical College, Dongguan 523808, China
e-mail: xuerongsun@126.com

X. Sun · H. Luo · S. Nie

Department of Physiology, Guangdong Medical College, Zhanjiang 524023, China

L. Chen (✉) · L. Zhu

Department of Pharmacology, Medical College, Jinan University, Guangzhou 510632, China
e-mail: chenlixinw@sohu.com

J. Mao

Department of Biology, Guangdong Key Laboratory for Bioactive Drugs Research, Guangdong Pharmaceutical University, Guangzhou 510006, China

L. Wang (✉)

Department of Physiology, Medical College, Jinan University, Guangzhou 510632, China
e-mail: wangliwei@sohu.com

Keywords Patch-clamp technique · Regulation of ion transport by cell volume · Ion channel/epithelial cell · Epithelial chloride transport

Introduction

Regulation of cell volume under osmotic challenges is one of the most fundamental functions of cellular homeostatic mechanisms. In response to osmotic swelling, most cells extrude cytoplasmic solutes, and water resulting in a regulatory volume decrease (RVD). Activation of volume-activated chloride channels and the consequent Cl^- efflux play a key role in the RVD in many cells (Chen et al. 2010; Harvey et al. 2010; Okada et al. 2009).

The characteristics of the volume-activated chloride current $I_{cl,vol}$ have been intensively investigated in many kinds of cells derived from different tissues (Chen et al. 2010; Inoue et al. 2010; Mao et al. 2010; Okada 2006). Besides cell volume regulation, the volume regulatory

chloride channels underpinning $I_{\text{cl,vol}}$ play extensive roles in various biological functions, including fluid secretion, maintenance of resting membrane potential, cell proliferation, and cell migration, among others (Mao et al. 2007; Okada et al. 2009).

Epithelial cells derived from the ectodermal blastoderm during embryonic development share many similar functions, such as barrier function and secretion, and activate $I_{\text{cl,vol}}$ in response to hypotonic challenges, except in normal cervical epithelial cells (Chou et al. 1995). We previously reported that fetal nasopharyngeal epithelial cells possess background chloride currents under isotonic conditions (Sun et al. 2005b), which implied potential physiological roles of the related channels in the cells. However, whether nasopharyngeal epithelial cells can produce $I_{\text{cl,vol}}$ under hypotonic conditions and whether the background chloride current and the $I_{\text{cl,vol}}$ share similar characteristics are still unknown.

During the development of the nasopharyngeal epithelium, cell proliferation and differentiation are vigorous; and the frequent flow of ions and water is necessary for these biological processes. Volume-activated chloride channels probably play an important role during the processes, though the characteristics of the $I_{\text{cl,vol}}$ in these cells have not been explored. In previous studies, we have explored the characteristics and roles of the $I_{\text{cl,vol}}$ in the human nasopharyngeal carcinoma cell line CNE-2Z (Chen et al. 2002, 2007). However, the $I_{\text{cl,vol}}$ in the counterpart of the carcinoma cell, the normal human nasopharyngeal epithelial cell, has not been investigated, mostly due to the difficulty in harvesting enough normal nasopharyngeal epithelial cells. In this study, we explored the characteristics of the $I_{\text{cl,vol}}$ in primary cultured fetal human nasopharyngeal epithelial cells.

Materials and Methods

Cell Preparation

Fetal human nasopharyngeal epithelial cells were prepared as previously described (Sun et al. 2005b). Briefly, nasopharyngeal epithelia were obtained from 4-month-old fetuses of induced labor. Dissected tissues were explanted onto round coverslips and supplied with Dulbecco's modified Eagle medium/F12 medium containing 5 ng/ml epidermal growth factor (PeproTech, Rocky Hill, NJ), 5×10^{-7} mol/l hydrocortisone (Sigma, St. Louis, MO) and 5 $\mu\text{g/ml}$ insulin (Sigma). Nasopharyngeal epithelial cells in primary culture of 1–2 weeks were used for experiments. The protocol of the study adhered to the tenets of the Declaration of Helsinki and was approved by the local ethics committee.

Electrophysiological Experiments

Whole-cell currents were recorded using the patch-clamp technique with a List EPC-7 patch-clamp amplifier (List Electronic, Darmstadt, Germany). Electrodes with 5–10 M Ω when filled with pipette solution were pulled from standard wall borosilicate glass capillaries. The liquid junction potential was corrected when the electrode entered the bath. After digitization at 3 kHz using a CED 1401 laboratory interface (CED, Cambridge, UK), voltage and current signals from the amplifier together with synchronizing pulses were stored in a computer. For the majority of experiments, cells were held at 0 mV and stepped to ± 40 , 0 and ± 80 mV for 200 ms with a 4 s interval repeatedly. Occasionally, the responses to stepwise (20 mV) pulses from -120 to $+120$ mV were examined. All current measurements were made 20 ms after the onset of each voltage pulse. All patch-clamp recordings were made at room temperature (20–24°C). Cell capacitance was detected using the methods described previously by us (Chen et al. 2002). Current density was obtained by dividing the current value with cell capacitance. The reversal potential of the current was calculated according to the linear equation $y = ax + b$, and the equilibrium potential for each ion was obtained from the Nernst formula.

Solutions and Chemicals

The pipette solution contained 70 mM *N*-methyl-D-glucamine chloride (NMDG-Cl), 1.2 mM MgCl₂, 10 mM HEPES, 1 mM EGTA, 140 mM D-mannitol, and 2 mM Na₂ATP. The isotonic bath solution contained 70 mM NaCl, 0.5 mM MgCl₂, 2 mM CaCl₂, 10 mM HEPES, and 140 mM D-mannitol. The osmolarity in the pipette and isotonic bath solutions was measured with a freezing-point osmometer (Osmomat 030; Gonotec, Berlin, Germany) and adjusted to 300 mOsm/l with D-mannitol. The hypotonic bath solution was obtained by omitting the D-mannitol from the solution, giving an osmolarity of 160 mOsm/l. In some experiments, the chloride channel blocker tamoxifen, 5-nitro-2-(3-phenylpropylamino) benzoic acid (NPPB) or ATP was added to hypotonic bath solutions to investigate their effects on hypotonicity-activated currents. Tamoxifen, NPPB, and ATP were purchased from Sigma-Aldrich (Poole, UK), and preparation of the stock solution was referred to the method previously described (Chen et al. 2002).

Anion Substitution Experiments

In anion substitution experiments, an agar bridge was used to connect the reference electrode to the bath solution. When the hypotonicity-activated current reached the peak and leveled off, 70 mM NaCl in the 47% hypotonic solution was

replaced by equimolar of NaI, NaBr, or sodium gluconate. The permeability ratio (P_X/P_{Cl}) of various anions relative to that of Cl⁻ was calculated using the modified Goldman-Hodgkin-Katz equation, $P_X/P_{Cl} = \{[Cl^-]_n \exp(-\Delta V_{rev} F/RT) - [Cl^-]_s\} / [X^-]_s$ (Chen et al. 2002), where $[Cl^-]_n$ and $[Cl^-]_s$ are the Cl⁻ concentration in the normal and the substituted bath solutions, $[X^-]_s$ is the concentration of the substituted anion, ΔV_{rev} is the difference of the reversal potentials for Cl⁻ and X⁻, F is the Faraday constant, R is the gas constant and T is the absolute temperature.

Statistics

Values are expressed as mean \pm standard error (number of observations). Analysis of variance (ANOVA) or Student's t -test was used to test for significant differences, and $P < 0.05$ was taken to be significant.

Results

I_{cl,vol} in Nasopharyngeal Epithelial Cells

Coverslips with fetal nasopharyngeal epithelial cells were placed in a perfusion recording chamber. Whole-cell currents were recorded using the patch-clamp technique. Cells were clamped at 0, ± 40 , and ± 80 mV (Fig. 1a). When cells were bathed in the isotonic solution, currents were small and stable (Fig. 1b). The current value at ± 80 mV was 0.16 ± 0.02 nA ($n = 23$). A large current was activated when cells were exposed to 47% hypotonic bath solution for 1–2 min (Fig. 1c). The current reached a peak and leveled off 3–5 min after exposure to hypotonic solution. Clamped cells remained in a swollen state in hypotonic

solution. When hypotonic bath solution was replaced with control isotonic solution, cells shrank toward normal size while the current declined gradually to the basal level. These results indicated that the hypotonicity-activated current was sensitive to cell volume changes.

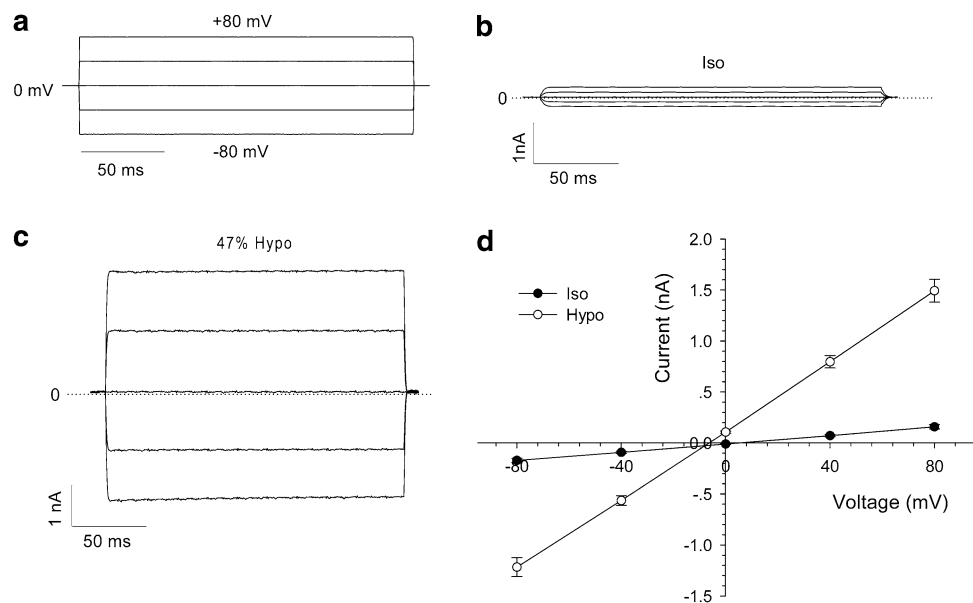
As shown in Fig. 1c, the hypotonicity-activated current presented mild outward rectification. There was no, or negligible, time-dependent inactivation of the current at +80 mV. When the voltage was stepped to +120 mV from -120 mV, the current still showed no obvious time-dependent inactivation (data not shown). The current–voltage relationships under isotonic and hypotonic conditions are shown in Fig. 1d. The reversal potential of the hypotonicity-activated current was -7.31 ± 0.64 mV ($n = 23$), which was close to the calculated equilibrium potential for Cl⁻. In our experiments, the concentration of Cl⁻ in pipette solution was almost equal to that in bath solution. The calculated equilibrium potential for Cl⁻ was -0.9 mV. The results suggest that the main component of the current was I_{cl,vol} (details in Discussion).

At +80 mV step, the peak values of the I_{cl,vol} displayed great variation, changing from 0.82 to 2.71 nA in the 23 cells detected. To analyze further the hypotonicity-activated currents recorded in different cells, the current was normalized with cell capacitance, which is directly correlated with the area of cell surface. The results showed that the density of the hypotonicity-activated current in most cells (18/23) was smaller than 60 pA/pF. Only five cells presented a current larger than 60 pA/pF.

Independence of I_{cl,vol} on Exogenous ATP

To investigate the dependence of I_{cl,vol} activation on ATP in fetal nasopharyngeal epithelial cells, ATP was excluded from

Fig. 1 Whole-cell currents under isotonic and 47% hypotonic conditions. **a** The voltage protocol used to generate the current traces in **(b)** and **(c)**. Cells were held at 0 mV and stepped to ± 40 , 0 and ± 80 mV for 200 ms with a 4 s interval repeatedly. The basal current recorded under isotonic conditions (*I_{iso}*) was small **(b)**, and exposure to 47% hypotonic bath solution (*Hypo*) activated a large current **(c)**. Current values were measured 20 ms after the start of each voltage pulse, and the current–voltage relationships under isotonic and hypotonic conditions are shown in **(d)** (mean \pm SE, $n = 23$)



the pipette solution. After the whole-cell configuration was formed, the cell was dialyzed with the ATP-free pipette solution for more than 3 min before exposure to 47% hypotonic bath solution. The results indicated that the volume-activated chloride channels could be activated by the hypotonic challenge in the absence of exogenous ATP (Fig. 2). A hypotonicity-induced chloride current was recorded with the pipette containing the ATP-free solution. The current possessed properties similar to those recorded in the presence of intracellular ATP. The current showed a mild outward rectification and was not inactivated in the observed period. The reversal potential of the current was -7.17 ± 1.05 mV ($n = 9$), which was close to the Cl^- equilibrium potential. There was no significant difference in the current density between the currents recorded in the presence and absence of ATP in the pipette solution ($P > 0.05$, Fig. 2c).

In addition, when ATP was omitted from the pipette solution, the $I_{\text{Cl,vol}}$ could still be activated repeatedly (Fig. 2b). However, the $I_{\text{Cl,vol}}$ activated a second time was

somewhat smaller than that the first time, whether ATP was included in or excluded from the pipette solution (Fig. 2a, b). We defined the ratio of the currents elicited between the second time and the first time as the “recovery ratio.” That is, recovery ratio (%) = (current density induced the second time/current density induced the first time) \times 100%. Results showed that when ATP was omitted from the pipette solution the recovery ratios ($65.3 \pm 5.0\%$ at +80 mV, $68.4 \pm 10.3\%$ at -80 mV, $n = 5$) were slightly smaller than those when ATP was included in the pipette solution ($82.5 \pm 6.3\%$ at +80 mV, $80.9 \pm 8.0\%$ at -80 mV, $n = 5$), but the differences were not significant ($P > 0.05$).

Inhibition of $I_{\text{Cl,vol}}$ by Extracellular ATP

ATP in high concentrations has been proven to be a strong blocker of chloride channels in nasopharyngeal carcinoma cells (Chen et al. 2002). To characterize the $I_{\text{Cl,vol}}$ further, the effect of extracellular ATP on the current was tested in

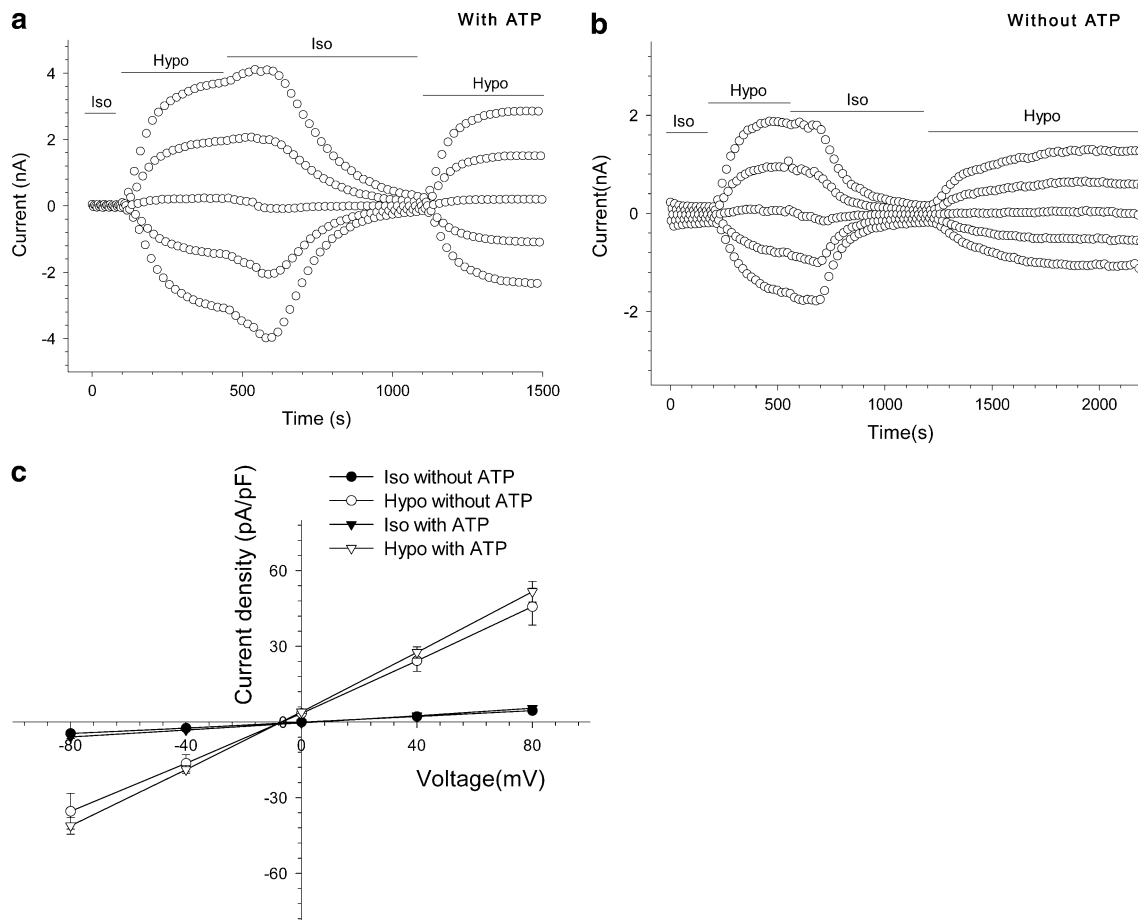


Fig. 2 Volume-activated chloride currents recorded with ATP-rich (2 mM) or ATP-free pipette solutions. Values of the whole-cell currents were obtained 20 ms after the start of each voltage step (0, ± 40 , and ± 80 mV). Large currents were activated repeatedly by the 47% hypotonic solution in both the presence (a) and the absence

(b) of ATP in the pipette solutions. The current–voltage relationships under isotonic (*Iso*) and hypotonic (*Hypo*) conditions with or without ATP in the pipette solution are shown in (c) (mean \pm SE of 11 cells without ATP or 23 cells with ATP). The difference in current density between the two groups was not significant

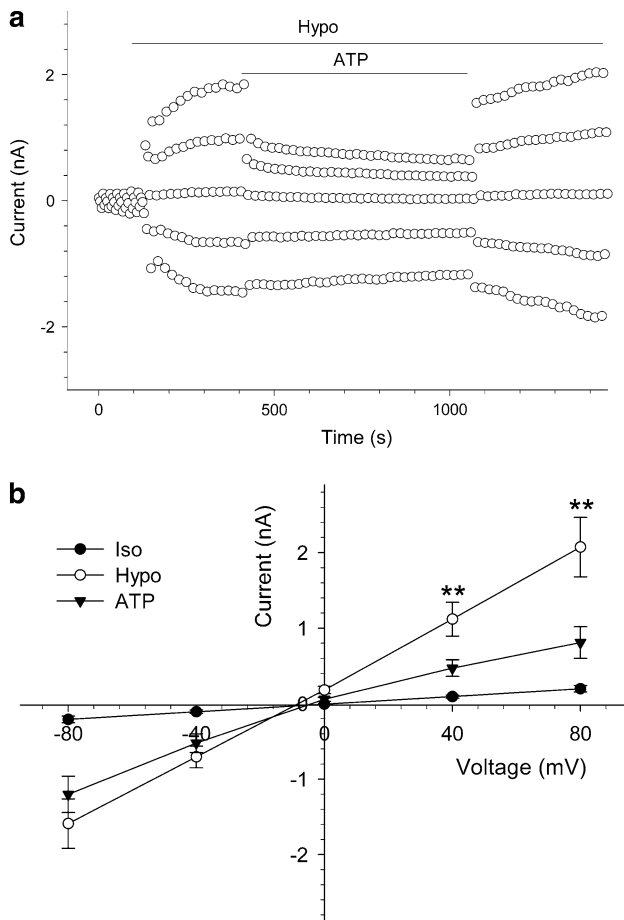


Fig. 3 Inhibition of volume-activated Cl^- currents by extracellular ATP. **a** Typical time course of volume-activated Cl^- currents induced by 47% hypotonic solution, indicated by the *Hypo* bar; and the effect of 10 mM extracellular ATP on the currents, indicated by the *ATP* bar. **b** Current–voltage relationships under isotonic (*Iso*) and hypotonic (*Hypo*) conditions and after treatment with the hypotonic solution containing 10 mM ATP (*ATP*). Data in (b) are mean \pm SE ($n = 7$). $**P < 0.01$ (vs. current value in ATP group)

fetal human nasopharyngeal epithelial cells. After $I_{\text{cl,vol}}$ were induced and leveled off, ATP was added to the hypotonic bath solution to a final concentration of 10 mM. As shown in Fig. 3, 10 mM ATP inhibited the $I_{\text{cl,vol}}$. The outward currents were more sensitive to ATP than the inward currents ($P < 0.01$). ATP (10 mM) inhibited $68.4 \pm 7.8\%$ ($P < 0.01$) of the outward current at +80 mV and only $22.8 \pm 8.2\%$ ($P > 0.05$) of the inward current at -80 mV ($n = 7$). The inhibitory effect of ATP was reversible upon washout.

Compared with the nasopharyngeal carcinoma cell line CNE-2Z (Chen et al. 2002), the inhibition effect of ATP on $I_{\text{cl,vol}}$ was much weaker in the current study. To confirm the difference, we investigated the effect of ATP on the background currents under isotonic conditions. Our recent research in nasopharyngeal carcinoma CNE-2Z cells showed that ATP at 10 mM could obviously inhibit the

background currents (Yang et al. 2011). Unexpectedly, in fetal nasopharyngeal epithelial cells, ATP at the same concentration activated an inward-rectification current. In six cells, ATP increased the inward current by 232.3 ± 64.3 pA at -80 mV and the outward current by 91.9 ± 35.0 pA at +80 mV (Fig. 4). The calculated reverse potential was +15.7 mV, which was far from the calculated Cl^- equilibrium potential. Furthermore, the chloride channel blockers NPPB (100 μM) and tamoxifen (20 μM) could not inhibit the inward-rectification current activated by ATP (Fig. 4e, f).

Sensitivity of $I_{\text{cl,vol}}$ to Tamoxifen

Figure 5a shows an example of the effect of tamoxifen, a Cl^- channel blocker, at 20 μM on the $I_{\text{cl,vol}}$. Tamoxifen (20 μM) inhibited $102.6 \pm 5.4\%$ of the outward current at +80 mV and $105.4 \pm 8.6\%$ of the inward current at -80 mV (Fig. 5b, $P < 0.01$, $n = 5$). The inhibition ratios on the outward and inward currents were similar ($P > 0.05$). The reason the inhibition ratios exceeded 100% was that tamoxifen not only inhibited $I_{\text{cl,vol}}$ completely but also inhibited the basic background currents (Sun et al. 2005b).

Inhibition of $I_{\text{cl,vol}}$ by Extracellular NPPB

NPPB is a classic chloride channel inhibitor. To explore its effect on $I_{\text{cl,vol}}$, NPPB was added into the perfusion solution after the activation of $I_{\text{cl,vol}}$. The results showed that $I_{\text{cl,vol}}$ was attenuated by extracellular applications of NPPB (Fig. 6). NPPB (100 μM) inhibited the $I_{\text{cl,vol}}$ by $45.48 \pm 9.02\%$ at +80 mV and $45.97 \pm 9.40\%$ at -80 mV ($n = 5$, $P < 0.01$). Increasing the concentration of NPPB to 200 μM further inhibited the $I_{\text{cl,vol}}$, with inhibition rates of $95.59 \pm 6.55\%$ at +80 mV and $86.95 \pm 9.61\%$ at -80 mV ($n = 5$, $P < 0.01$). At either 100 or 200 μM , NPPB inhibited outward and inward currents to similar degrees ($P > 0.05$).

It should be noted that NPPB, at a concentration of 200 μM , could obviously accelerate the time-dependent inactivation of the $I_{\text{cl,vol}}$ at +80 mV (Fig. 6c). This phenomenon could hardly be detected in the application of ATP, tamoxifen and low-concentration NPPB (100 μM).

Permeability of Volume-Activated Chloride Channels

When the $I_{\text{cl,vol}}$ was activated and had reached a peak, the hypotonic solution containing 70 mM of Cl^- was replaced with hypotonic solution containing equimolar I^- , Br^- or gluconate. The anion substitution shifted the reversal potential. The permeability ratios of $P_{\text{I}}/P_{\text{Cl}}$, $P_{\text{Br}}/P_{\text{Cl}}$, and $P_{\text{gluconate}}/P_{\text{Cl}}$ calculated from the shifts in reversal potential by the modified Goldman-Hodgkin-Katz equation are

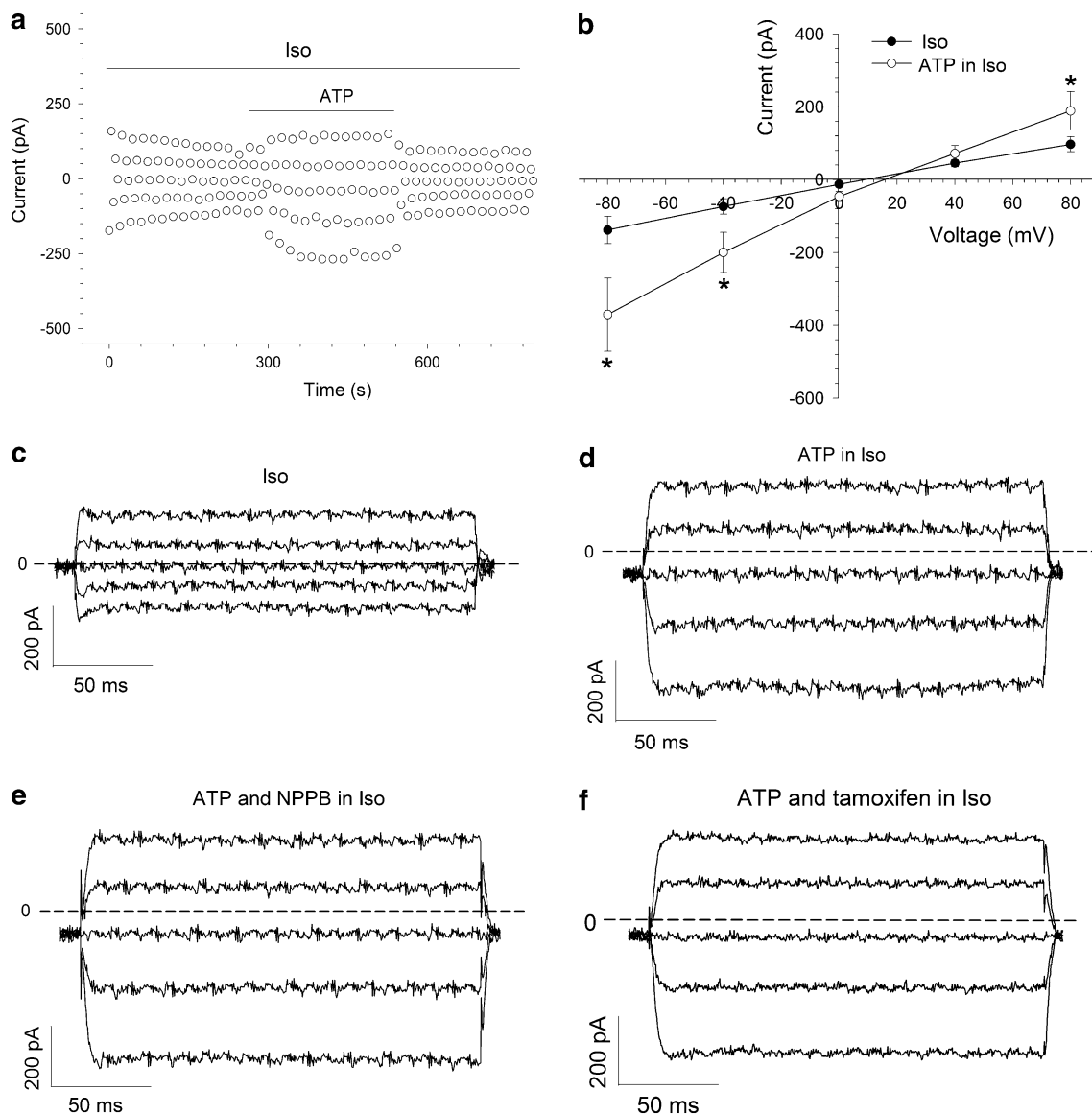


Fig. 4 Currents activated by 10 mM ATP in isotonic conditions. A typical time course of the ATP-activated, inward-rectified current in isotonic solution (*Iso*) is shown in (a). The current declined upon ATP washout. Current–voltage relationships of the background current in the isotonic solution and the ATP-activated current are presented in

shown in Fig. 7. The sequence of anion permeability was $\text{I}^- > \text{Br}^- > \text{Cl}^- > \text{gluconate}$.

Discussion

The current study demonstrated that hypotonic challenges activated a volume-sensitive current in fetal human nasopharyngeal epithelial cells. The current direction and reversal potential for the current were consistent with those of the current carried by Cl^- . The sensitivity to chloride channel blockers and the anion permeability of the

(b) (mean \pm SE, $n = 6$). c–f Typical current traces of the background current in isotonic solution (c), inward-rectified current activated by ATP (d) and effects of NPPB (100 μM) (e), and tamoxifen (20 μM) (f) on the ATP-activated current. * $P < 0.05$ (vs. current value in *Iso* group)

channels were similar to the $I_{\text{Cl,vol}}$ recorded in other cells (Inoue et al. 2005; Stutzin and Hoffmann 2006). Therefore, fetal human nasopharyngeal epithelial cells can produce $I_{\text{Cl,vol}}$ under hypotonic conditions.

The $I_{\text{Cl,vol}}$ in this study shared most of the characteristics with the background chloride current recorded by us previously under isotonic conditions in fetal nasopharyngeal epithelial cells (Sun et al. 2005b). Our recent research suggests that both the background chloride current and the $I_{\text{Cl,vol}}$ in nasopharyngeal carcinoma CNE-2Z cells are mediated by the same volume-activated chloride channels (Yang et al. 2011); the volume-activated chloride channels

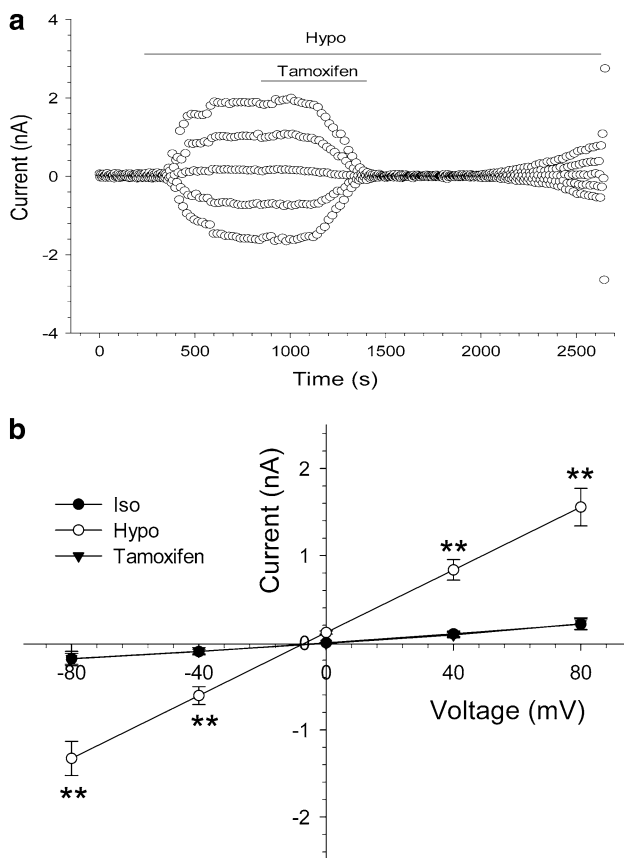


Fig. 5 Inhibition of volume-activated Cl^- currents by the chloride channel blocker tamoxifen. **a** Typical time course of the volume-activated Cl^- current induced by 47% hypotonic solution, indicated by the *Hypo* bar; and the effect of 20 μM extracellular tamoxifen on the current, indicated by the *Tamoxifen* bar. **b** Current–voltage relationships under isotonic (*Iso*) and hypotonic (*Hypo*) conditions and after treatment with the hypotonic solution containing 20 μM tamoxifen (*Tamoxifen*). Data in (**b**) are mean \pm SE ($n = 5$). $**P < 0.01$ (vs. current value in tamoxifen group)

in fetal nasopharyngeal epithelial cells probably underpins both the $I_{\text{Cl,vol}}$ in hypotonic conditions and the background chloride currents in isotonic conditions (Sun et al. 2005b). A functional role of the channels should exist in both hypotonic and isotonic conditions.

Our previous work indicated that the fetal human nasopharyngeal epithelial cells swelled and underwent a process of RVD when exposed to a hypotonic challenge (Sun et al. 2005a). Inhibition of the RVD by the chloride channel blockers ATP, NPPB and tamoxifen suggests a fundamental role of the volume-sensitive chloride channels in RVD (Sun et al. 2005a). The current study validates that $I_{\text{Cl,vol}}$ can be activated by the same hypotonic challenge and can also be inhibited by ATP, NPPB, and tamoxifen. Besides, the degree of inhibition of the chloride channel blockers on the RVD is similar to that on $I_{\text{Cl,vol}}$ presented in the current study. These results confirm that the $I_{\text{Cl,vol}}$ plays a key role in the RVD in fetal human nasopharyngeal epithelial cells.

Based on the morphology described by us previously (Sun et al. 2005a), cultured fetal nasopharyngeal epithelial cells were heterogeneous, mainly due to their dynamic and asynchronous development. It is well known that all somatic cells are derived from stem cells. During the process of histogenesis, a few self-renewing stem cells give rise to a limited number of committed progenitors. Progenitor cells have limited proliferation ability, subsequently differentiate into precursor cells, and eventually become terminally mature cells (Alison et al. 2006). Therefore, the primary cultured nasopharyngeal epithelial cells in the current study might be a mixture of stem cells, progenitor cells, precursor cells, and fully differentiated mature cells.

On the basis of current density of $I_{\text{Cl,vol}}$ and cell size distribution, our results in this study reveal that the current density and cell size vary greatly among the cells observed; but the exact significance of the variation remains to be clarified in future studies. It has been reported that stem or progenitor cells usually display smaller size relative to the corresponding mature cells (De Paiva et al. 2006; Greene et al. 2010; Izumi et al. 2009) and that the primitive immature cells, such as progenitor cells or tumor cells, generally possessed stronger $I_{\text{Cl,vol}}$ compared with the differentiated ones (Chou et al. 1995; Qian et al. 2009; Voets et al. 1997). Thus, it is possible that the variation of current density may be caused by the difference of the stages of cells situated. It should be noted that cell cycle distribution and cell apoptosis also have great influence on both cell size and current density (Chen et al. 2002; Stutzin and Hoffmann 2006; Zuo et al. 2009). Therefore, these factors should be taken into account in future research.

Most reports indicate that the activation of $I_{\text{Cl,vol}}$ depends on intracellular ATP (Okada et al. 2009; Poletto Chaves and Varanda 2008; Stutzin and Hoffmann 2006). However, the degree of dependence is variable under different conditions. A study on rat IMCD cells showed that intracellular ATP was necessary to evoke $I_{\text{Cl,vol}}$ when the hypotonic stimulus was modest but was not when the stimulus was stronger (Volk et al. 1996). In N1E115 neuroblastoma cells and human prostate cancer epithelial cells, the results suggest that volume-sensitive Cl^- channels can be activated via two different mechanisms, i.e., ATP-dependent and ATP-independent mechanisms, and that increasing the rate of cell swelling appears to increase the proportion of channels activated via the ATP-independent pathway (Bond et al. 1999; Lazarenko et al. 2005). In our study, deletion of ATP from the pipette solution did not significantly change the original activation, the current density, and the repeated activation (embodied by the recovery ratio) of $I_{\text{Cl,vol}}$, suggesting that exogenous ATP seems to be not necessary for activation of $I_{\text{Cl,vol}}$. However, our results do not exclude the dependence of $I_{\text{Cl,vol}}$ on endogenous ATP. The first reason is that the production of ATP by the clamped cells was not inhibited by the

Fig. 6 Inhibition of volume-activated chloride currents by the chloride channel blocker NPPB. Cells were clamped at 0, ± 40 and ± 80 mV for 200 ms with an interval of 4 s. **a–c** Typical current traces recorded in 47% hypotonic control solution (**a**) and in 47% hypotonic solution containing 100 μM (**b**), or 200 μM NPPB (**c**), respectively. **d** Time course of activation of $I_{\text{Cl,vol}}$ induced by 47% hypotonic challenge (*Hypo*) and inhibition of the current by 100 and 200 μM NPPB. NPPB inhibited $I_{\text{Cl,vol}}$ in a dose-dependent manner and obviously accelerated the time-dependent inactivation at $+80$ mV in higher concentrations (**c**)

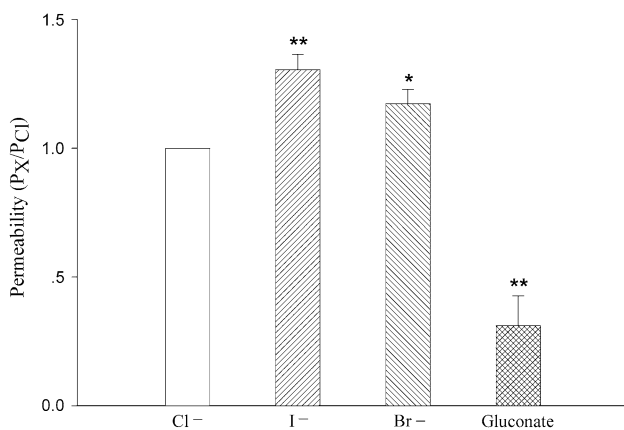
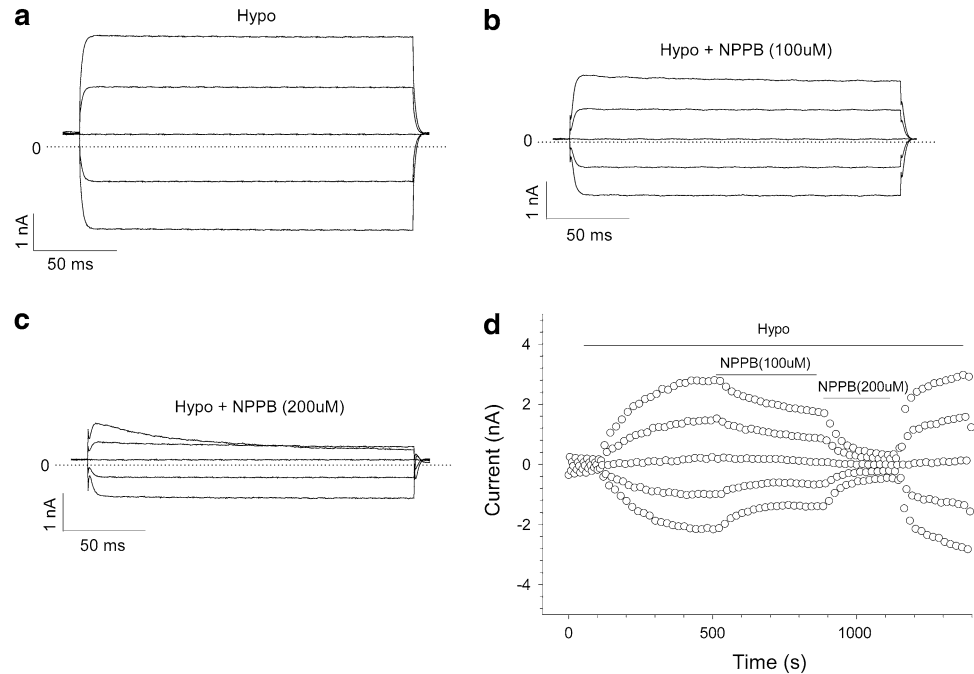


Fig. 7 Anion permeability of volume-activated chloride channels. The permeability ratios (P_X/P_{Cl}) of various anions (X^-), including I^- , Br^- , and gluconate, relative to Cl^- were calculated as described in **Materials and Methods**. Data represent mean \pm SE ($n = 5$). ** $P < 0.01$ and * $P < 0.05$, respectively (vs. Cl^-)

metabolic inhibitors, as in other reports (Bond et al. 1999; Lazarenko et al. 2005). The second is that the 47% hypotonic bath solution used in our study represents a strong hypotonic stimulus, which would induce cell swelling at a high rate and, thus, might activate the $I_{\text{Cl,vol}}$ mainly through the ATP-independent pathway (Bond et al. 1999).

The $I_{\text{Cl,vol}}$ in fetal nasopharyngeal epithelial cells shared many similar characteristics with those in nasopharyngeal carcinoma cells (Chen et al. 2002). However, under isotonic conditions, 10 mM ATP activated an inward-rectified current in fetal nasopharyngeal epithelial cells, which has not been observed in nasopharyngeal carcinoma cells

(Yang et al. 2011). The reversal potential of the ATP-activated current ($+15.7$ mV) was far from the Cl^- equilibrium potential. The current showed inward rectification and was insensitive to NPPB and tamoxifen. All of these characteristics are different from those of the $I_{\text{Cl,vol}}$, the cAMP-activated chloride current or the Ca^{2+} -activated chloride current (Morris 1999). Therefore, the ATP-activated current should not be mediated by Cl^- . Based on the ion concentration in the pipette and the bath solution, the equilibrium potential of Na^+ is $+73.5$ mV and the equilibrium potential of Mg^{2+} is -11.2 mV. Both are far from the reversal potential. Therefore, the ATP-activated current is probably mediated mainly by Ca^{2+} , though the coexistence of a magnesium current cannot be excluded. Activation of the ATP-activated current might be mediated by the ionotropic purinoceptor P2X (Browne et al. 2010), which needs to be explored further. In this study, the mild inhibition of ATP on the $I_{\text{Cl,vol}}$ might be the conjunct result of the inhibition of $I_{\text{Cl,vol}}$ and the activation of cation currents. Since the ATP (10 mM)-activated current could not be observed in nasopharyngeal carcinoma CNE-2Z cells (Yang et al. 2011), the current study implies that normal fetal nasopharyngeal epithelial cells and nasopharyngeal carcinoma cells might have a great difference in the expression of purinergic receptors.

The molecular identity of $I_{\text{Cl,vol}}$ is still unknown. Several proteins, including pIcln, CIC-3, and P-glycoprotein (the MDR1 gene product), have been described as possible molecular candidates. However, many results suggest that these proteins might only be channel regulators, not the real channels (Okada 2006; Verkman and Galletta 2009). CIC-3

belongs to the highly evolutionarily conserved CIC family. Our previous studies in nasopharyngeal carcinoma cells have shown that CIC-3 is a key protein in the activation of I_{cl,vol} and that CIC-3 is also a main component of the background chloride channels activated under isotonic conditions (Mao et al. 2008; Wang et al. 2004; Yang et al. 2011). The role of CIC-3 in fetal nasopharyngeal epithelial cells is not clear and will be one of the targets of our next study.

As a summary, our study demonstrated that, in response to hypotonic challenges, fetal human nasopharyngeal epithelial cells could produce I_{cl,vol}, which was sensitive to the chloride channel inhibitors and independent of exogenous ATP. Compared with nasopharyngeal carcinoma CNE-2Z cells, ATP displayed a weaker inhibition of I_{cl,vol} in fetal nasopharyngeal epithelial cells, due to the activation of another inward-rectified current.

Acknowledgments This work was supported by the National Natural Science Foundation of China (30771106, 30870567, 30871267, 90913020 and U0932004) and the Science & Technology Innovation Fund of Guangdong Medical College (STIF201102).

References

- Alison MR, Brittan M, Lovell MJ, Wright NA (2006) Markers of adult tissue-based stem cells. *Handb Exp Pharmacol* 174:185–227
- Bond T, Basavappa S, Christensen M, Strange K (1999) ATP dependence of the I_{Cl}, swell channel varies with rate of cell swelling. Evidence for two modes of channel activation. *J Gen Physiol* 113:441–456
- Browne LE, Jiang LH, North RA (2010) New structure enlivens interest in P2X receptors. *Trends Pharmacol Sci* 31:229–237
- Chen L, Wang L, Zhu L, Nie S, Zhang J, Zhong P, Cai B, Luo H, Jacob TJ (2002) Cell cycle-dependent expression of volume-activated chloride currents in nasopharyngeal carcinoma cells. *Am J Physiol Cell Physiol* 283:C1313–C1323
- Chen LX, Zhu LY, Jacob TJ, Wang LW (2007) Roles of volume-activated Cl⁻ currents and regulatory volume decrease in the cell cycle and proliferation in nasopharyngeal carcinoma cells. *Cell Prolif* 40:253–267
- Chen B, Jefferson DM, Cho WK (2010) Characterization of volume-activated chloride currents in regulatory volume decrease of human cholangiocyte. *J Membr Biol* 235:17–26
- Chou CY, Shen MR, Wu SN (1995) Volume-sensitive chloride channels associated with human cervical carcinogenesis. *Cancer Res* 55:6077–6083
- De Paiva CS, Pflugfelder SC, Li DQ (2006) Cell size correlates with phenotype and proliferative capacity in human corneal epithelial cells. *Stem Cells* 24:368–375
- Greene SB, Gunaratne PH, Hammond SM, Rosen JM (2010) A putative role for microRNA-205 in mammary epithelial cell progenitors. *J Cell Sci* 123:606–618
- Harvey VL, Saul MW, Garner C, McDonald RL (2010) A role for the volume regulated anion channel in volume regulation in the murine CNS cell line, CAD. *Acta Physiol (Oxf)* 198:159–168
- Inoue H, Mori S, Morishima S, Okada Y (2005) Volume-sensitive chloride channels in mouse cortical neurons: characterization and role in volume regulation. *Eur J Neurosci* 21:1648–1658
- Inoue H, Takahashi N, Okada Y, Konishi M (2010) Volume-sensitive outwardly rectifying chloride channel in white adipocytes from normal and diabetic mice. *Am J Physiol Cell Physiol* 298:C900–C909
- Izumi K, Inoki K, Fujimori Y, Marcelo CL, Feinberg SE (2009) Pharmacological retention of oral mucosa progenitor/stem cells. *J Dent Res* 88:1113–1118
- Lazarenko RM, Kondrats'kyi AP, Pohoriela N, Shuba IM (2005) Alterations in ATP dependence of swelling-activated Cl⁻ current associated with neuroendocrine differentiation of LNCaP human prostate cancer epithelial cells [in Russian]. *Fiziol Zh* 51:57–66
- Mao J, Wang L, Fan A, Wang J, Xu B, Jacob TJ, Chen L (2007) Blockage of volume-activated chloride channels inhibits migration of nasopharyngeal carcinoma cells. *Cell Physiol Biochem* 19:249–258
- Mao J, Chen L, Xu B, Wang L, Li H, Guo J, Li W, Nie S, Jacob TJ, Wang L (2008) Suppression of CIC-3 channel expression reduces migration of nasopharyngeal carcinoma cells. *Biochem Pharmacol* 75:1706–1716
- Mao J, Xu B, Li H, Chen L, Jin X, Zhu J, Wang W, Zhu L, Zuo W, Chen W, Wang L (2010) Lack of association between stretch-activated and volume-activated Cl⁻ currents in hepatocellular carcinoma cells. *J Cell Physiol* 226:1176–1185
- Morris AP (1999) The regulation of epithelial cell cAMP- and calcium-dependent chloride channels. *Adv Pharmacol* 46:209–251
- Okada Y (2006) Cell volume-sensitive chloride channels: phenotypic properties and molecular identity. *Contrib Nephrol* 152:9–24
- Okada Y, Sato K, Numata T (2009) Pathophysiology and puzzles of the volume-sensitive outwardly rectifying anion channel. *J Physiol* 587:2141–2149
- Poletto Chaves LA, Varanda WA (2008) Volume-activated chloride channels in mice Leydig cells. *Pflugers Arch* 457:493–504
- Qian JS, Pang RP, Zhu KS, Liu DY, Li ZR, Deng CY, Wang SM (2009) Static pressure promotes rat aortic smooth muscle cell proliferation via upregulation of volume-regulated chloride channel. *Cell Physiol Biochem* 24:461–470
- Stutzin A, Hoffmann EK (2006) Swelling-activated ion channels: functional regulation in cell-swelling, proliferation and apoptosis. *Acta Physiol (Oxf)* 187:27–42
- Sun XR, Chen LX, Mao JW, Zhu LY, Nie SH, Zhong P, Li P, Wang LW (2005a) Regulatory volume decrease and its mechanism in nasopharyngeal epithelial cells [in Chinese]. *Shi Yan Sheng Wu Xue Bao* 38:353–358
- Sun XR, Wang LW, Mao JW, Zhu LY, Nie SH, Zhong P, Chen LX (2005b) Background chloride currents in fetal human nasopharyngeal epithelial cells [in Chinese]. *Sheng Li Xue Bao* 57:349–354
- Verkman AS, Galiotta LJ (2009) Chloride channels as drug targets. *Nat Rev Drug Discov* 8:153–171
- Voets T, Wei L, De Smet P, Van Driessche W, Eggermont J, Droogmans G, Nilius B (1997) Downregulation of volume-activated Cl⁻ currents during muscle differentiation. *Am J Physiol Cell Physiol* 272:C667–C674
- Volk KA, Zhang C, Husted RF, Stokes JB (1996) Cl⁻ current in IMCD cells activated by hypotonicity: time course, ATP dependence, and inhibitors. *Am J Physiol Renal Physiol* 271:F552–F559
- Wang LW, Chen LX, Jacob T (2004) CIC-3 expression in the cell cycle of nasopharyngeal carcinoma cells. *Sheng Li Xue Bao* 56:230–236
- Yang L, Ye D, Ye W, Jiao C, Zhu L, Mao J, Jacob TJ, Wang L, Chen L (2011) CIC-3 is a main component of background chloride channels activated under isotonic conditions by autocrine ATP in nasopharyngeal carcinoma cells. *J Cell Physiol* 226:2516–2526
- Zuo W, Zhu L, Bai Z, Zhang H, Mao J, Chen L, Wang L (2009) Chloride channels involve in hydrogen peroxide-induced apoptosis of PC12 cells. *Biochem Biophys Res Commun* 387:666–670